Calibration of the polarimeter POMME at proton energies between 1.05 and 2.4 GeV

N.E. Cheung [a], C.F. Perdrisat [a,*], J. Oh [a], K. Beard [a], V. Punjabi [b], J. Yonnet [c],
R. Beurtey [c], M. Boivin [c], F. Plouin [c], E. Tomasi-Gustafsson [c], A. Boudard [d], R. Abegg [e],
V. Ladygin [f], L. Penchev [f], N. Piskunov [f], I. Sitnik [f], E.A. Strokovsky [f], S. Belostotsky [g],
V. Vikhrov [g], R. Frascaria [h], B. Johnson [h], R. Siebert [h], E. Warde [h], W.W. Jacobs [i],
W.T.H. van Oers [j], C. Lippert [k], S. Nanda [l]

[a] The College of William and Mary, Williamsburg, VA 23185, USA
[b] Norfolk State University, Norfolk, VA 23504, USA
[c] Laboratoire National Saturne, DSM-CEA et CNRS-IN2P3 CE Saclay, 91191 Gif-sur-Yvette Cedex, France
[d] DSM-CEA / DAPNIA / SPhN, CE Saclay, 91191 Gif-sur-Yvette Cedex, France
[e] TRIUMF, Vancouver, British Columbia, Canada T6G 2J1
[f] LHE, JINR, Dubna, Russian Federation
[g] LNPI, Gatchina, Russian Federation
[h] IPN, CNRS-IN2P3, Orsay, France
[i] IUCF, Bloomington, Indiana 47405, USA
[j] University of Manitoba, Winnipeg, Manitoba, Canada R3T 2N2
[k] University of Bonn, W-5300 Bonn 1, Germany
[l] CEBAF, Newport News, VA 23606, USA

Received 2 November 1994

Abstract

We report a new calibration of the polarimeter POMME for energies between 1.05 and 2.40 GeV using polarized proton beams at the Laboratoire National Saturne. A 16 parameter and a new 14 parameter empirical formula have been used to fit both the angular and energy dependencies of the inclusive proton–carbon analyzing power data between 0.80 and 2.40 GeV. Both fits have very good chi-square, 1.20 per degree of freedom for the former, and 1.05 for the latter. The parameters from these fits can be used to predict the angular distribution of the pC analyzing power at any energy within the energy range of the fits.

1. Introduction

Polarization experiments have recently become increasingly important in the study of nuclear reactions such as (d, p) and (e, e'p). The measurement of spin observables for hadronic and electromagnetic interactions provides a rich source of information about nuclear structure and spin-dependent forces. Polarization measurements in the focal plane of a magnetic spectrometer have become a well established and very important experimental technique in these type of investigations. The focal plane polarimeter POMME (Polarimètre Mobile à Moyenne Energie) at the Laboratoire National Saturne was built for such purpose.

POMME was first calibrated in 1988 for proton kinetic energies between 0.20 and 1.20 GeV using the spectrometer SPES I. The results of this calibration have been published by Bonin et al. [1].

In the course of a recent investigation of the polarization transfer from deuteron to proton in both the inclusive deuteron breakup reaction and the backward dp elastic scattering, it became necessary to extend the POMME calibration up to 2.40 GeV. The results of this new calibration also have great interest at CEBAF (Continuous Electron Beam Acceleration Facility) where a large focal plane polarimeter is being installed in the 4 GeV/c high resolution hadron spectrometer in Hall A.

The new calibration was accomplished in two separate runs, first in 1990 and then in 1992, using the spectrometer SPES IV [2,3]. Polarized proton beams with seven different energies were used; 1.6 and 1.8 GeV in 1990, and

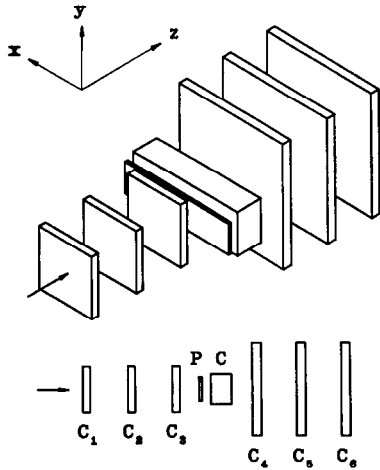* Corresponding author. Tel. +1 804 221 3572, fax +1 804 221 3540.

Fig. 1. Schematic diagram of the polarimeter POMME. C_1, C_2 and C_3 are the small front chambers. C_4, C_5 and C_6 are the large rear chambers. C is the carbon analyzer and P is the plastic scintillator. Also shown is the coordinate system used here.

1.05, 1.35, 2.00, 2.24 and 2.40 GeV in 1992. In this paper we report the results of this calibration. In the next section, we describe the working principle of POMME and show some representative characteristics of a proton polarimeter. The calibration proper is described in Section 3. In Section 4, results for a new 14 parameter fit of the proton–carbon analyzing power, and an old Los Alamos 16 parameter fit [4] based on a previously published function [5] are given. A discussion of the results is presented in the final section.

2. Polarimeter principle and characteristics

The polarization of medium energy protons can be determined by scattering the protons with an analyzer, typically made of carbon or liquid hydrogen, and measuring the azimuthal angular distribution of the scattered particles. A complete description of the polarimeter POMME has been published elsewhere [1,6], including its special MWPC readout system using the charge division method. Here, we only mention briefly the basic working principle of POMME and some of its characteristics. The device contains six XY multiwire proportional chambers and a thick carbon block as the analyzer. A schematic diagram of POMME is shown in Fig. 1. The working principle is based on inclusive proton–carbon scattering, with one forward charged particle detected,

$$p + C \rightarrow \text{one forward charged particle} + X. \quad (1)$$
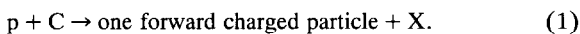
The three small upstream chambers, C_1, C_2 and C_3, seen in Fig. 1, have a sensitive area of 48×48 cm², while the sensitive areas for the three large downstream chambers, C_4, C_5, and C_6, are 96×96 cm². The chambers permit the particle trajectory reconstruction both before and after

the pC scattering, and so give the measurement of the scattering angles.

The three small front chambers have an average spatial resolution of 1.6 mm (FWHM), and the resolution for the large chambers is 3.2 mm (FWHM). Taking into account the redundancy of the three-chamber system, the overall trajectory reconstruction efficiency we measured is 99.8% for the small chamber group, and 85% for the large chamber group. The carbon analyzer, C, used in POMME had a thickness of 53.0 g cm⁻², comparable with the carbon nuclear collision length, which is 60.2 g cm⁻². The probability of having any pC nuclear interaction in POMME was then given by $[1 - \exp(-53.0/60.2)] = 0.59$. A plastic scintillator, P, was placed between the small front chambers and the carbon analyzer, and it served as part of the POMME trigger.

In the energy region where the C(p,p)X reaction dominates the pC interactions, the forward going charged particles are mostly protons. In general, their angular distribution after the analyzer has the form of

$$n(\theta, \phi) = n_0(\theta)\{1 + A_{pC}(\theta)[P_y \cos \phi - P_x \sin \phi]\}, \quad (2)$$

where n_0 is the distribution for unpolarized protons, and $A_{pC}(\theta)$ is the analyzing power of carbon in POMME that we would like to calibrate. P_y and P_x are the projections of the proton polarization onto the vertical- and horizontal-axis, respectively. The angles θ and ϕ are the polar and azimuthal scattering angles of the protons, respectively. As shown in Eq. (2), once the proton beam polarization is known, the analyzing power, A_{pC}, can be found by Fourier analysis of the angular distribution of the scattered protons.

3. Calibration

The polarimeter was calibrated with a polarized proton beam. First, we had to determine the proton beam polarization, and then we used the polarized beam to measure the POMME analyzing power. This process was repeated for each beam energy at which we made the measurement.

For the beam polarization measurements, the spectrometer SPES IV was set at an angle θ_{lab} relative to the incoming beam, and a liquid hydrogen target was put in place in front of SPES IV. The angles θ_{lab} used for different beam energies and the corresponding proton–proton analyzing powers determined by Perrot et al. [7] are given in Table 1.

During the experiment, the spin of the proton beam was orientated in the vertical direction and flipped between up and down for consecutive beam bursts. The spectrometer at angle θ_{lab} together with the hydrogen target acted as a single-arm polarimeter using proton–proton scattering. The hodoscopes located at the intermediate and final focal

Table 1
Results for the measurements of the proton beam polarization, P_p, at various energies, as well as the pp scattering angles, θ_{lab}, and the analyzing powers, A_{pp}, that were used. The uncertainties in P_p given are statistical only, and included the statistical errors propagated from A_{pp} [5]

T_p [GeV]	θ_{lab} [deg]	A_{pp}	P_p
1.05	16.1	0.420 ± 0.020	0.885 ± 0.045
1.35	16.1	0.360 ± 0.020	0.875 ± 0.050
1.60	10.1	0.330 ± 0.030	0.860 ± 0.080
1.80	10.1	0.295 ± 0.020	0.855 ± 0.060
2.00	13.9	0.270 ± 0.020	0.815 ± 0.060
2.24	13.9	0.235 ± 0.020	0.810 ± 0.070
2.40	11.6	0.255 ± 0.020	0.765 ± 0.060

plane of SPES IV detected the scattered protons. The measured asymmetry, X, is given by

$$X(\theta_{lab}) = \frac{N_\uparrow - N_\downarrow}{N_\uparrow + N_\downarrow}, \qquad (3)$$

where $N_\uparrow$ and $N_\downarrow$ are the number of protons counted in SPES IV with the beam polarization in the spin-up and spin-down state, respectively. One also has

$$X(\theta_{lab}) = P_p A_{pp}(\theta_{lab}), \qquad (4)$$

where A_{pp} is the pp analyzing power at angle θ_{lab}, and P_p is the proton beam polarization to be determined.

The results of the P_p measurements at various energies are given in Table 1. The statistical uncertainties of P_p include the root sum square of the contributions from both the $X(\theta_{lab})$ measurement and the statistical error in $A_{pp}(\theta_{lab})$. According to Ref. [7], the systematic error of A_{pp} was estimated to be 4% over the energy range relevant here. This results in an additional 4% systematic uncertainty in the proton beam polarization measurements which is not included in Table 1.

After the beam polarization had been determined, the liquid hydrogen target was removed. The polarized proton beam entered the spectrometer at 0° and was then guided onto the polarimeter POMME at the final focal plane of SPES IV. In the energy range of our calibration, the pC scattering at small angle is dominated by the multiple Coulomb scattering which has a typical scattering angle of 0.6° (rms). All protons not undergoing any nuclear interaction in the carbon appear in this "Coulomb peak". These events have no analyzing power and are therefore useless for polarization measurements. Besides, the azimuthal angular resolution of POMME is poor when θ is less than 1°. Events with small θ were rejected on-line to reduce both the computer dead-time and the amount of magnetic tapes needed to store the data.

During the calibration, the electronic signals from the wire chambers and other detectors were sent to the data acquisition computer SAR [8]. The signals from the chambers C_1, C_3 and C_6 were read first and the information

was used to estimate the polar scattering angle, θ, of the pC scattering. A fast-rejection test was run by SAR to reject events with θ smaller than 2°. One percent of the raw events were collected without going through this test, providing a sample of the original "uncensored" event population. If an event passed this small angle test, SAR continued to read the remaining information from other detectors, and transferred the data onto a magnetic tape for off-line analysis. Otherwise, the system was reset and ready for the next event.

During off-line analysis, the particle trajectories both before and after the carbon analyzer were reconstructed event by event, using the information from all six wire chambers. Only single track events were selected. The coordinates of the proton scattering vertex in the carbon and the scattering angles, θ and ϕ, were then calculated. Software windows were used to select events that had vertex coordinates compatible with the location of the analyzer. A cone-test was used to remove the instrumental asymmetry originating from the finite size of the chambers behind the analyzer. For an event with a given polar scattering angle θ, this test required that the whole 2π azimuthal acceptance for the scattered particle be contained within the large chambers located after the carbon analyzer.

Events that passed the cone-test and the software windows were used to determine the analyzing power of the carbon analyzer, $A_{pC}(\theta)$. The angular distribution of the events are shown in Fig. 2 for the 1.60 GeV data. A strongly suppressed Coulomb peak at θ less than 2° is visible in Fig. 2(a). These are mostly events from the 1% "uncensored" data. The ϕ distribution shown in Fig. 2b displays a clear cosine modulation.

Since the direction of the beam polarization of consecutive beam bursts was alternated between up and down in
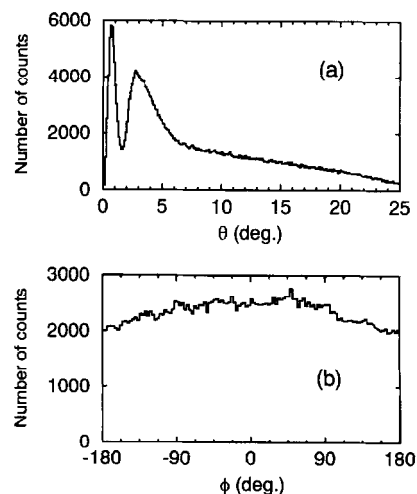

Fig. 2. (a) The θ-distribution and (b) the ϕ-distribution of the scattered particles at 1.60 GeV.

the vertical direction throughout the experiment, we have

$$n_\uparrow(\theta, \phi) = n_0(\theta)\{1 + P_{\mathrm{p}} A_{\mathrm{pC}}(\theta) \cos \phi\},$$

$$n_\downarrow(\theta, \phi) = n_0(\theta)\{1 - P_{\mathrm{p}} A_{\mathrm{pC}}(\theta) \cos \phi\}, \qquad (5)$$

where $n_\uparrow$ and $n_\downarrow$ are the distributions for the proton spin-up and spin-down state, respectively. The asymmetry, $R(\theta, \phi)$, of the proton angular distribution after the carbon analyzer is given by

$$R(\theta, \phi) = \frac{n_\uparrow(\theta, \phi) - n_\downarrow(\theta, \phi)}{n_\uparrow(\theta, \phi) + n_\downarrow(\theta, \phi)}$$

$$= P_{\mathrm{p}} A_{\mathrm{pC}}(\theta) \cos \phi. \qquad (6)$$

After Fourier analysis of $R(\theta, \phi)$, one has

$$R(\theta, \phi) = A_0(\theta) + A_1(\theta) \cos \phi + B_1(\theta) \sin \phi + \cdots. \qquad (7)$$

All coefficients except A_1 are expected to be zero. The typical values of B_1 were found to be plus or minus 0.01 ± 0.01, and are indeed compatible with zero. Comparing Eqs. (6) and (7), we have

$$A_{\mathrm{pC}}(\theta) = A_1(\theta)/P_{\mathrm{p}}. \qquad (8)$$

The results of the A_{pC} calibration, together with the statistical uncertainties are given in Table 2. There is a 4% systematic uncertainty in A_{pC}, which comes from the

proton beam polarization measurements, as mentioned above.

Besides the analyzing power, the figure of merit, F, is also a very important quantity characterizing a polarimeter. It is defined as

$$F^2 \equiv \int_{\theta_{\min}}^{\theta_{\max}} \frac{n_0(\theta)}{N_{\mathrm{inc}}} A_{\mathrm{pC}}^2(\theta) \, d\theta, \qquad (9)$$

with N_{inc} the total number of incoming protons; $(\theta_{\min}, \theta_{\max})$ indicates the useful scattering angle domain of the polarimeter. The absolute statistical uncertainty of the polarization measured by a polarimeter is simply given by

$$\Delta P_{\mathrm{p}} \simeq \sqrt{2/F^2 N_{\mathrm{inc}}}. \qquad (10)$$

The figure of merit provides a very important guideline to determine the number of events one has to acquire during an experiment to achieve a given absolute uncertainty for the measurement. The values of F, integrated from 3° to 25°, are given in Table 3 at various proton energies. The value at 1.05 GeV is consistent with the earlier result from Ref. [1]. Also given in Table 3 and Fig. 3 are the figure of merit after correction for the chamber efficiency so that the new values correspond to a POMME like polarimeter with chambers of 100% detection efficiency.

A very important aspect of the figure of merit as defined here is that it depends not only on the hardware of

Table 2

Values of the proton–carbon analyzing power, $A_{\mathrm{pC}}(\theta)$, obtained in this experiment at various proton kinetic energies. The uncertainties given are statistical only. The systematic uncertainties are 4%, as discussed in the text

θ [deg]	$A_{\mathrm{pC}}(\theta)$						
	1.05 GeV	1.35 GeV	1.60 GeV	1.80 GeV	2.00 GeV	2.24 GeV	2.40 GeV
3	0.136 ± 0.010	0.123 ± 0.010	0.109 ± 0.013	0.096 ± 0.010	0.092 + 0.011	0.087 + 0.012	0.084 ± 0.012
4	0.163 ± 0.011	0.152 ± 0.011	0.136 ± 0.016	0.110 ± 0.011	0.124 ± 0.014	0.098 ± 0.014	0.118 ± 0.016
5	0.186 ± 0.012	0.168 ± 0.013	0.119 ± 0.015	0.137 ± 0.014	0.118 ± 0.015	0.140 ± 0.018	0.098 ± 0.017
6	0.195 ± 0.013	0.177 ± 0.014	0.137 ± 0.018	0.131 ± 0.014	0.130 ± 0.016	0.130 ± 0.018	0.124 ± 0.018
7	0.190 ± 0.013	0.183 ± 0.015	0.155 ± 0.019	0.124 ± 0.014	0.123 ± 0.016	0.120 ± 0.018	0.098 ± 0.018
8	0.209 ± 0.014	0.169 ± 0.014	0.157 ± 0.020	0.118 ± 0.014	0.138 ± 0.017	0.122 ± 0.019	0.107 ± 0.019
9	0.205 ± 0.014	0.186 ± 0.015	0.122 ± 0.018	0.137 ± 0.015	0.121 ± 0.017	0.092 ± 0.018	0.089 ± 0.019
10	0.209 ± 0.015	0.191 ± 0.015	0.128 ± 0.019	0.114 ± 0.015	0.129 ± 0.018	0.100 + 0.019	0.085 ± 0.020
11	0.202 ± 0.014	0.165 ± 0.015	0.121 ± 0.019	0.103 ± 0.015	0.108 ± 0.017	0.097 ± 0.019	0.087 ± 0.020
12	0.200 ± 0.014	0.164 ± 0.015	0.134 ± 0.020	0.107 ± 0.015	0.107 ± 0.018	0.153 ± 0.022	0.057 ± 0.020
13	0.208 ± 0.015	0.172 ± 0.015	0.131 ± 0.020	0.133 ± 0.017	0.146 ± 0.020	0.076 ± 0.020	0.067 ± 0.021
14	0.210 ± 0.015	0.177 ± 0.016	0.095 ± 0.019	0.120 ± 0.017	0.096 ± 0.019	0.093 ± 0.021	0.152 ± 0.025
15	0.193 ± 0.014	0.160 ± 0.015	0.104 ± 0.019	0.120 ± 0.017	0.066 ± 0.019	0.059 ± 0.021	0.033 ± 0.023
16	0.202 ± 0.015	0.146 ± 0.015	0.087 ± 0.019	0.093 ± 0.017	0.081 ± 0.020	0.074 ± 0.022	0.081 ± 0.024
17	0.181 ± 0.014	0.168 ± 0.016	0.083 ± 0.019	0.071 ± 0.017	0.083 ± 0.020	0.055 ± 0.022	0.072 ± 0.025
18	0.181 ± 0.015	0.165 ± 0.016	0.088 ± 0.020	0.070 ± 0.017	0.098 ± 0.021	0.077 ± 0.023	0.052 ± 0.026
19	0.176 ± 0.015	0.140 ± 0.016	0.101 ± 0.022	0.069 ± 0.018	0.031 ± 0.021	0.050 ± 0.023	0.035 ± 0.026
20	0.191 ± 0.015	0.100 ± 0.015	0.102 ± 0.022	0.078 ± 0.019	0.062 ± 0.021	0.009 ± 0.024	0.019 ± 0.027
21	0.177 ± 0.015	0.126 ± 0.016	0.098 ± 0.023	0.023 ± 0.019	0.069 ± 0.022	0.013 ± 0.025	0.047 ± 0.029
22	0.157 ± 0.015	0.122 ± 0.018	0.057 ± 0.023	0.050 ± 0.020	0.053 ± 0.024	0.043 ± 0.026	0.004 ± 0.029
23	0.171 ± 0.016	0.119 ± 0.019	0.092 ± 0.026	0.040 ± 0.022	0.032 ± 0.026	0.024 ± 0.027	0.011 ± 0.033
24	0.133 ± 0.017	0.074 ± 0.021	0.030 ± 0.028	0.032 ± 0.024	0.058 ± 0.029	0.067 ± 0.031	0.079 ± 0.038
25	0.152 ± 0.019	0.095 ± 0.025	0.003 ± 0.032	0.034 ± 0.028	0.037 ± 0.033	−0.028 ± 0.035	0.005 ± 0.043

Table 3
The figure of merit of POMME, integrated from $\theta = 3°$ to 25°. The numbers in the second column are experimental results from POMME. In the third column are results after corrected for the chamber detection efficiency, as described in the text. The error bars given are statistical only

T_p [GeV]	Figure of merit, F (10^{-2})	
	POMME	Corrected for efficiency
1.05	9.45 ± 0.15	10.26 ± 0.17
1.35	5.75 ± 0.12	6.24 ± 0.13
1.60	3.96 ± 0.15	4.30 ± 0.16
1.80	4.23 ± 0.13	4.60 ± 0.15
2.00	4.28 ± 0.16	4.65 ± 0.17
2.24	3.66 ± 0.16	3.98 ± 0.18
2.40	2.90 ± 0.15	3.15 ± 0.17

Table 4
The values of p_{mid} and the thickness of the carbon analyzer used at different proton energies

T_p [GeV]	p_{mid} [GeV/c]	Thickness [cm]
0.80	1.40	31.2
1.05	1.69	31.2
1.20	1.86	30.0
1.35	2.03	31.2
1.60	2.30	31.2
1.80	2.52	31.2
2.00	2.73	31.2
2.24	2.98	31.2
2.40	3.15	31.2

the polarimeter, but also on the beam quality and the way events were selected during analysis. In this calibration, we used a monochromatic proton beam that was directed onto the center of the carbon analyzer. On the other hand, if the beam was not monochromatic and the spectrometer spreads the protons over the analyzer, more events would be rejected by the cone-test mentioned above and the figure of merit could be reduced significantly.

4. Parametrization

4.1. 14 parameter fitting

A 14 parameter empirical formula was used to fit the energy and angular dependences of the obtained data between 0.80 and 2.40 GeV; besides the seven sets of data reported here, two more sets of data from a previous calibration, at 0.80 and 1.20 GeV, were also included in the fit. The fitting formula consists of two exponential functions and has the following form:

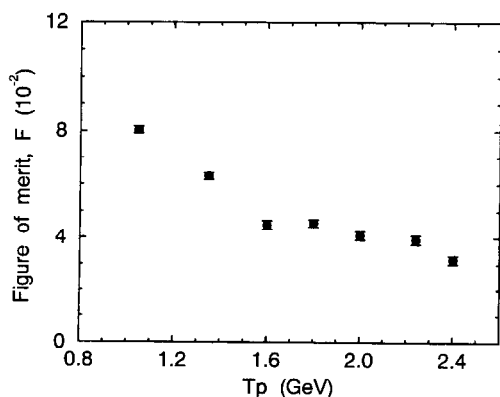$$A_{pC}(\theta, p_{mid}) = ax^r e^{-bx} + cx^s e^{-dx} \qquad (11)$$

with $x = p_{mid}\sin \theta$, where p_{mid} is the proton momentum in GeV/c at the middle of the carbon analyzer after correction for the energy loss. The thickness of the carbon analyzer was 31.2 cm for all data sets, except at 1.20 GeV where the thickness was 30.0 cm. The reason p_{mid} was used is to reduce the analyzer thickness dependence to a simple momentum dependence. The values of p_{mid} together with the thickness of the carbon analyzer used at different proton energies are given in Table 4. The six quantities a, b, c, d, r and s, are parametrized functions given as:

$$a = a_0 + a_1 p' + a_2 p'^2,$$
$$b = b_0 + b_1 p' + b_2 p'^2,$$
$$c = c_0 + c_1 p' + c_2 p'^2, \qquad (12)$$
$$d = d_0 + d_1 p' + d_2 p'^2,$$
$$r = r_0,$$
$$s = s_0,$$

where

$$p' = p_{mid} - 2.3 \text{ GeV}/c.$$

The new momentum variable p' was chosen to be at the center of the parametrization domain.

Eq. (11) and the above parametrized functions were used to fit the A_{pC} data between $\theta = 3°$ and 25°. Nine sets of data, a total of 207 data points, were included. The optimum values of the 14 parameters as well as their

Fig. 3. The figure of merit of POMME, integrated from $\theta = 3°$ to 25° and corrected for the chamber detection efficiency.

Table 5
The optimum values for the 14 parameter fit of the inclusive pC analyzing power data

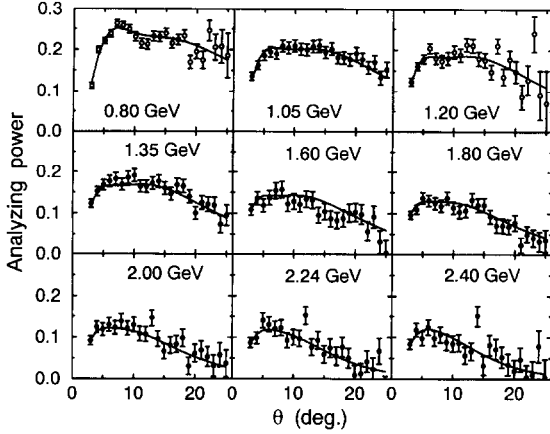|	0	1	2
a	5758 ± 6665	-9910 ± 12289	4543 ± 5997
b	26.45 ± 3.14	-7.018 ± 1.957	-3.448 ± 1.399
c	6.015 ± 3.029	-4.492 ± 2.855	3.654 ± 2.564
d	4.676 ± 0.561	-0.2947 ± 0.2357	0.6398 ± 0.3732
r	3.869 ± 0.419		
s	2.066 ± 0.321		

Fig. 4. Results of the 14 parameter fit of the inclusive proton–carbon analyzing power, A_{pC}. The curves are from the fit. The filled circles are data from this work and the open circles are results from the previous calibration of Ref. [1].

uncertainties are given in Table 5. The fit, obtained with the code MINUIT, has a very good chi-square of 1.05 per degree of freedom. The curves from the fit are compared with the calibration data in Fig. 4. The results of this proton-carbon analyzing power parametrization between 0.80 and 2.40 GeV are plotted in Fig. 5 in steps of 0.20 GeV. The curves show that the pC analyzing power has its peak at θ between 5° and 10°. As the proton energy increases, the value of A_{pC} decreases from roughly 0.22 at 0.80 GeV to about 0.10 at 2.40 GeV. This trend indicates that the analyzing power is likely to become even smaller at proton energies beyond 2.40 GeV.

4.2. 16 parameter fitting

In the previous calibration [1], a 16 parameter formula, first proposed by Ransome et al. [5], was used to fit the analyzing power of POMME between 0.5 and 1.2 GeV. Such a fit has been used by McNaughton et al. [4] at the Los Alamos National Laboratory to parametrize the pC analyzing power below 1.2 GeV. It is interesting to see how well this 16 parameter fit works in the newly calibrated energy region, and to compare it with the results from the 14 parameter fit we have presented above. The 16 parameter fit is based on the analytical form

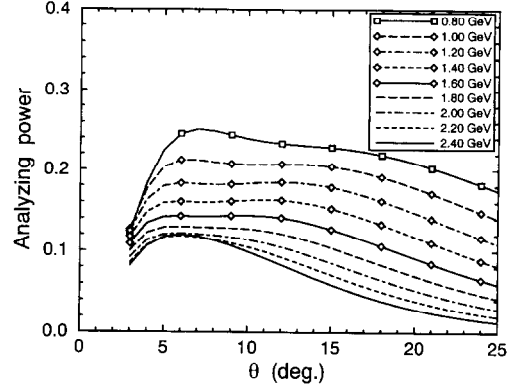$$A_{pC}(\theta, p_{mid}) = \frac{ax}{1 + bx^2 + cx^4} + dp_{mid}\sin(5\theta), \quad (13)$$

Fig. 5. The parametrized inclusive pC analyzing power between $T_p = 0.80$ and 2.40 GeV, from the 14 parameter fit.

with $x = p_{mid}\sin\theta$. The quantities a, b, c and d are parametrized as follows:

$$a = a_0 + a_1 p' + a_2 p'^2 + a_3 p'^3$$
$$b = b_0 + b_1 p' + b_2 p'^2 + b_3 p'^3 \quad (14)$$
$$c = c_0 + c_1 p' + c_2 p'^2 + c_3 p'^3$$
$$d = d_0 + d_1 p' + d_2 p'^2 + d_3 p'^3$$

where

$$p' = p_{mid} - 2.3 \text{ GeV}/c.$$

The fitting prescription was applied to the same nine sets of calibration data over the same θ range between 3° and 25° as described above for the 14 parameter fitting. The resulting values for the 16 parameters of the optimum fit are given in Table 6. The fit gives a chi-square of 1.20 per degree of freedom, slightly higher than the 14 parameter fit. Fig. 6 shows the 16 parameter fit with the calibration data. The results between 0.80 and 2.40 GeV are shown in Fig. 7 in steps of 0.20 GeV. At energies between 0.80 and 1.40 GeV, both fits show a similar behavior. At higher energies, the curves from the 16 parameter fit start to cross each other.

5. Discussion

We have reported the first systematic measurement of the high energy inclusive proton–carbon analyzing power. The old Los Alamos 16 parameter fit and a new 14
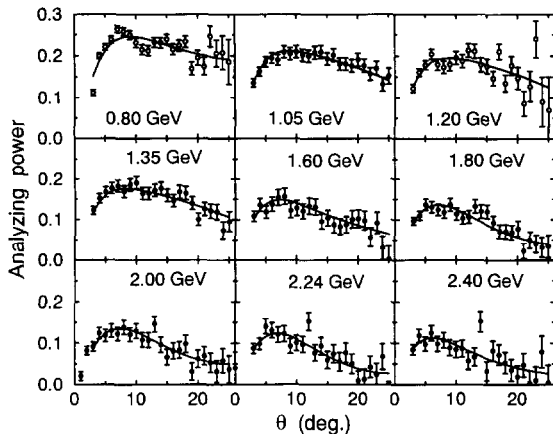
Table 6
The optimum values for the 16 parameter fit of the inclusive pC analyzing power data

	0	1	2	3
a	0.9791 ± 0.0534	−0.4707 ± 0.1389	0.5810 ± 0.1230	−0.5966 ± 0.2504
b	11.31 ± 1.62	−19.63 ± 3.97	5.421 ± 2.429	13.79 ± 5.84
c	6.204 ± 3.959	−13.38 ± 10.54	−12.92 ± 5.78	31.41 ± 16.03
d	0.00497 ± 0.00811	−0.1012 ± 0.0114	0.00116 ± 0.01267	0.1285 ± 0.0256

Fig. 6. Results of the Los Alamos 16 parameter fit of the inclusive proton–carbon analyzing power, A_{pC}. The curves are from the fit. The filled circles are data from this work and the open circles are results from the previous calibration of Ref. [1].

parameter fit were used to parametrize the results for energies between 0.80 and 2.40 GeV. Both fits describe the analyzing power well, but the 14 parameter fit has a smoother behaviour at energies beyond 1.40 GeV. As the energy increases, both the analyzing power A_{pC} and the figure of merit F of the polarimeter POMME decrease. At 2.40 GeV, A_{pC} becomes as small as 0.1 and F is about 3×10^{-2}. Thus for polarized protons with higher energies,
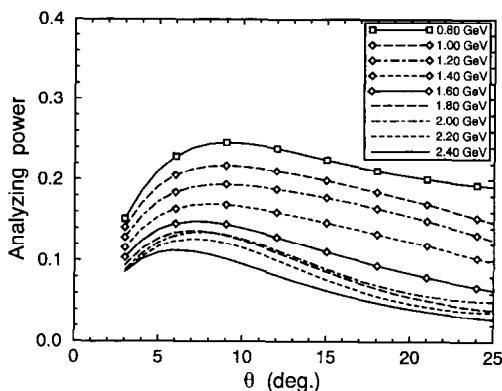

Fig. 7. The parametrized inclusive pC analyzing power between $T_p = 0.80$ and 2.40 GeV, from the Los Alamos 16 parameter fit explained in the text.

it will become necessary to use other reactions with larger analyzing power for proton polarimetry. A possibility might be C(p, 2p)X [9] or some other exclusive pC interactions, although these reactions require particle identification and energy measurement after the analyzer. Other options have been investigated using materials such as copper [9], hydrogen [10,11] or deuterium [12] as the analyzer. The simplest choice would be liquid hydrogen since the pp analyzing power, A_{pp}, is about three times larger than A_{pC} in the high energy region [10]. Of course, its relatively low density $(0.0708 \text{ g cm}^{-3})$ and the necessity to have a cryogenic system will certainly be a challenge to the designers of the next generation of high energy proton polarimeters.

Acknowledgements

References

[1] B. Bonin et al., Nucl. Instr. and Meth. A 288 (1990) 379.
[2] E. Grorud, J.L. Laclare, A. Ropert, A. Tkatchenko, J. Banaigs and M. Boivin, Nucl. Instr. and Meth. 188 (1981) 549.
[3] M. Bedjidian et al., Nucl. Instr. and Meth. A 257 (1987) 132.
[4] M.W. McNaughton et al., Nucl. Instr. and Meth. A 241 (1985) 435.
[5] R.D. Ransome et al., Nucl. Instr. and Meth. 201 (1982) 315.
[6] E. Tomasi-Gustafsson, POMME – Polarimetre Mobile Moyenne Energie manual, LNS/Ph/92-07 Centre National de la Recherche Scientifique.
[7] F. Perrot et al., Nucl. Phys. B 294 (1987) 1001.
[8] Laboratoire National Saturne, SARI manual, Laboratoire National Saturne, 1990.
[9] C. Ohmori et al., Phys. Lett. B 243 (1990) 29.
[10] H. Spinka et al., Nucl. Instr. and Meth. 211 (1983) 239.
[11] E. Tomasi-Gustafsson, J. Yonnet and V. Ladygine, LNS/Ph/94-07 Centre National de la Recherche Scientifique.
[12] C. Ohmori et al., Phys. Lett. B 230 (1989) 27.